A New Family of π-Conjugated Delocalized Biradicals: Electronic Structures of 1,4-Bis(2,5-diphenylimidazol-4-ylidene)cyclohexa-2,5-diene

Azusa Kikuchi,[†] Hiroaki Ito,[‡] and Jiro Abe*[,†]

Department of Chemistry, and The 21st Century COE Program, Aoyama Gakuin University, 5-10-1 Fuchinobe, Sagamihara, Kanagawa 229-8558, Japan, and Department of Photo-Optical Engineering, Tokyo Institute of Polytechnics, Kanagawa 243-02, Japan

Received: April 28, 2005; In Final Form: August 8, 2005

A new family of π-conjugated delocalized biradical compound is developed. The solution of 1,4-bis(2,5-diphenylimidazol-4-ylidene)cyclohexa-2,5-diene shows the ESR signal consisting of a moderately broad unresolved line, $\Delta H_{pp} \approx 1$ mT, at room temperature. The presence of the thermal equilibrium between a triplet biradical state and a singlet state is confirmed by the ESR measurements, and the spin concentration is determined as 7.90×10^{21} spin/mol at 300 K. The spin concentration can also be controlled by modifying the molecular planarity. Moreover, the unrestricted DFT/B3LYP calculations suggest the biradical character of the singlet ground state, and the modulation of the energy gap between the singlet state and the triplet state is investigated from the theoretical point of view. Controlling the equilibrium between a diamagnetic state and a paramagnetic state will provide significant progress in the field of biradical chemistry, and the materials with the biradical character in a ground state will lead to a novel development of molecular-based organic magnets.

1. Introduction

Oxidation of 2,4,5-triarylimidazole gives 2,4,5-triarylimidazolyl radical, showing the radical recombination reaction to form 2,2′,4,4′,5,5′-hexaarylbiimidazole (HABI) (Scheme 1a).[1] Because 2,4,5-triphenylimidazole has the common name lophine, HABIs and 2,4,5-triarylimidazolyl radicals are sometimes called lophine dimers and lophyl radicals, respectively. Lophine is also known as the first chemiluminescence materials discovered by Radziszewsky in 1877.[1b] HABIs are well-known photochromic compounds and have been applied to a free radical initiator in photopolymer imaging for more than three decades.[2l−n] There are a number of spectroscopic studies for the photochemical reaction of HABI and their derivatives.[2] We have already reported an unprecedented example of the in situ direct observation of a light-induced radical pair in a single crystal of *o*-Cl-HABI by X-ray diffraction, and we described the first example of the measurement of intermolecular exchange coupling for the radical pair by ESR measurement.[3] On the other hand, the bisimidazole derivative, 1,4-bis(4,5-diphenylimidazole-2-ylidene)cyclohexa-2,5-diene (BDPI-2Y), does not show the radical dimerization reaction. BDPI-2Y was first prepared by Zimmermann et al. in 1966 and was obtained as deep greenish-blue fine prisms with metallic luster.[4] Six years later, Sakaino et al. reported the temperature dependence of ESR signal intensities arising from a paramagnetic component in the powdered crystals of BDPI-2Y.[5] The paramagnetic component was ascribed to the triplet biradicals populated by the thermal excitation from a closed-shell ground state. That is, the presence of the thermal equilibrium between a diamagnetic closed-shell quinoidal ground state and a paramagnetic thermally excited biradical state had been considered for the origin of the temperature-dependent ESR signals (Scheme 1b). However, the population of the paramagnetic species of BDPI-2Y in solution is negligibly small at room temperature due to the large energy gap between a diamagnetic ground state and a paramagnetic triplet excited state.

SCHEME 1: (a) Photochromic Reaction of HABI, (b) Thermal Equilibrium between a Biradical Form and a Quinoidal Form in BDPI-2Y, and (c) Thermal Equilibrium between a Biradical Form and a Quinoidal Form in BDPI-4Y

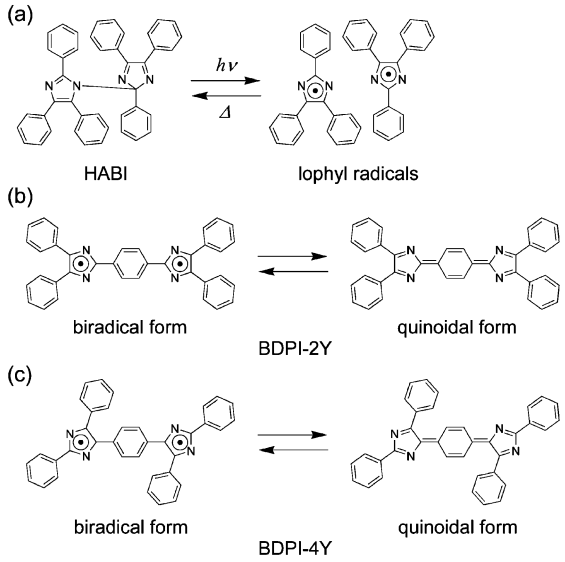

Recently, we have reported a novel BDPI-2Y derivative, tF-BDPI-2Y, substituted four hydrogen atoms at the central phenylene ring of BDPI-2Y with fluorine atoms (Scheme 2).[6] The increase in the population of biradical species of tF-BDPI-2Y as compared to BDPI-2Y in solution was achieved, and the

* To whom correspondence should be addressed. E-mail: jiro_abe@chem.aoyama.ac.jp.
[†] Aoyama Gakuin University.
[‡] Tokyo Institute of Polytechnics.

10.1021/jp052207q CCC: $30.25
Published on Web 09/22/2005

SCHEME 2: Thermal Equilibrium between a Biradical Form and a Quinoidal Form in tF-BDPI-2Y and the Photochromic Reaction of tF-BDPI-2YD

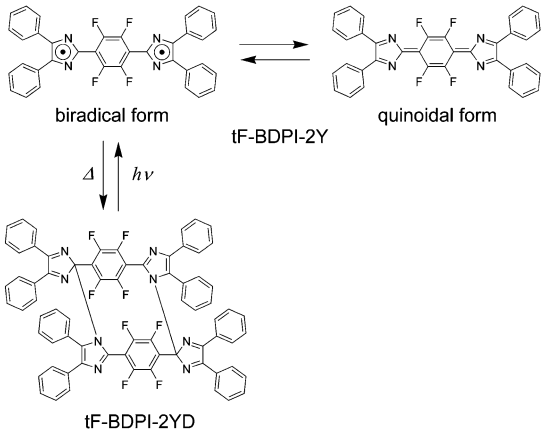

formation of a dimer of tF-BDPI-2Y, tF-BDPI-2YD, was confirmed by the X-ray diffraction study. Moreover, tF-BDPI-2YD shows a photochromic reaction characteristic of HABIs. Our investigation could give the definitive evidence for the presence of a biradical state in tF-BDPI-2Y. In the course of these studies, we came up with an idea that controlling the equilibrium between a closed-shell quinoidal state and an open-shell biradical state will provide significant progress in the field of biradical chemistry, and π-conjugated triplet biradicals can be applicable as spin-source units for molecular-based magnetic materials.

In this work, we have developed a new family of π-conjugated delocalized biradical compound, 1,4-bis(2,5-diphenylimidazole-4-ylidene)cyclohexa-2,5-diene (BDPI-4Y), which is a structural isomer of BDPI-2Y (Scheme 1c). The presence of the thermal equilibrium between a paramagnetic biradical state and a diamagnetic quinoidal state can be expected by analogy with BDPI-2Y. Our previous DFT/6-31G(d) calculations predicted a planar geometry for the closed-shell quinoidal state for BDPI-2Y.[6] As a matter of course, the quinoidal state of BDPI-2Y is most strongly stabilized when the two imidazolyl rings and the central phenylene ring lie on the same plane. However, these three rings in BDPI-4Y can never be coplanar due to a steric hindrance. The deviation from the planarity in BDPI-4Y as compared to BDPI-2Y can be expected to stabilize the energy level of the triplet biradical state and destabilize that of the closed-shell quinoidal state, resulting in a lowering of the energy gap between a diamagnetic ground state and a paramagnetic triplet biradical state.

2. Experimental Section

Materials. All reactions were performed under dry nitrogen atmosphere unless otherwise specified. Materials were purchased from TCI and Wako and used without further purification. BDPI-4Y derivatives were prepared following Scheme 3.

1,4-Bis(2,5-diphenylimidazol-4-ylidene)cyclohexa-2,5-diene (BDPI-4Y). (i) Under nitrogen, to a stirred solution of benzaldehyde (2.70 g, 25.7 mmol), 1,4-bisbenzil (4.00 g, 11.7 mmol) and ammonium acetate (18.0 g, 234 mmol) in acetic acid (200 mL) were heated to reflux, giving a light yellow and clear solution. After being refluxed for 12 h, the reaction mixture was cooled to room temperature and then added dropwise to an ice 10 % ammonia solution. A pale-yellow precipitate immediately formed and was collected by filtration and washed with water and then ethanol. Recrystallization of the pale-yellow product from pyridine gave 1,4-bis(2,5-diphenylimidazol-4-yl) benzene (BDPI-4Y-lophine) in 86% yield (5.2 g) as a white powder. ^{1}HNMR (DMSO-d_6, 500 MHz): δ 12.68 and 12.75 (s, 2H), 8.09 (s, 4H), 7.23−7.63 (m, 20H). IR (KBr) ν_{max}: 3401, 3062, 1604, 1512, 1488, 1461, 1410, 1129, 967, 913, 847, 775, 768, 696 cm^{-1}. FAB MS (*m*/*z*): $[M + H]^+$ calcd for $C_{36}H_{26}N_4$, 514.62; found, 515. Anal. Calcd for $C_{36}H_{26}N_4$: C, 84.02; H, 5.09; N, 10.89. Found: C, 84.02; H, 5.08; N, 10.90.

(ii) To a solution of BDPI-4Y-lophine (1.00 g, 1.94 mmol) in benzene (200 mL) containing aqueous potassium hydroxide (2 N, 400 mL) was added potassium ferricyanide (15.0 g, 38.0 mmol) in a period of 0.5 h. After addition of potassium ferricyanide, the organic layer became a blue solution from a colorless solution. The reaction mixture was stirred for an additional 2 days at room temperature. The organic layer was separated, washed with water, dried over calcium chloride, and concentrated to give 1,4-bis(2,5-diphenylimidazol-4-ylidene)-cyclohexa-2,5-diene(BDPI-4Y) as greenish-blue powder. Recrystallization from hot benzene gave BDPI-4Y in 73% yield (0.725 g) as deep greenish-blue microcrystals with metallic luster. IR (KBr) ν_{max}: 3059, 1597, 1558, 1481, 1437, 1387, 1348, 1321, 1292, 1278, 1258, 1172, 1120, 1066, 1052, 1020, 923, 773, 711, 697, 672 cm^{-1}. Anal. Calcd for $C_{36}H_{24}N_4$: C, 84.35; H, 4.72; N, 10.93. Found: C, 83.92; H, 4.70; N, 10.87.

SCHEME 3: Synthetic Procedure of BDPI-4Y Derivatives[a]

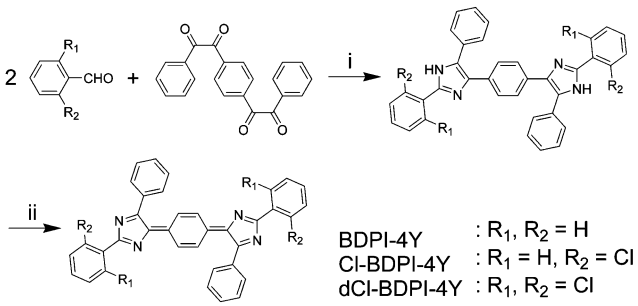

[a] (i) BDPI-4Y, 1,4-bisbenzil, $CH_3COONH_4-CH_3COOH$, 130 °C, 12 h (86%); Cl-BDPI-4Y, 1,4-bisbenzil, $CH_3COONH_4-CH_3COOH$, 130 °C, 2 days (70%); dCl-BDPI-4Y, 1,4-bisbenzil, $CH_3COONH_4-CH_3COOH$, 130 °C, 2 days (68%); (ii) BDPI-4Y, $K_3[Fe(CN)_6]$, KOHaq−benzene, rt, 2 days (73%); Cl-BDPI−4Y, $K_3[Fe(CN)_6]$, KOHaq−benzene, rt, 2 days (56%); dCl-BDPI−4Y, $K_3[Fe(CN)_6]$, KOHaq−benzene, rt, 2 days (51%).

1,4-Bis[2-(2-chlorophenyl)-5-phenylimidazol-4-ylidene]cyclohexa-2,5-diene (Cl-BDPI-4Y). (i) Under nitrogen, to a stirred solution of 2-chlorobenzalaldehyde (1.80 g, 12.8 mmol), 1,4-bisbenzil (2.00 g, 5.84 mmol) and ammonium acetate (10.0 g, 130 mmol) in acetic acid (200 mL) were heated to reflux, giving a light yellow and clear solution. After being refluxed for 2 days, the reaction mixture was cooled to room temperature and then added dropwise to an ice 10 % ammonia solution. It immediately formed a pale-yellow precipitate, which was collected by filtration and washed with water and then ethanol. Recrystallization of the pale-yellow product from pyridine gave 1,4-bis[(2-chlorophenyl)-5-phenyl-imidazol-4-yl)benzene (Cl-BDPI-4Y-lophine) in 70% yield (2.41 g) as a white powder. ^{1}HNMR (DMSO-d_6, 500 MHz): δ 12.53 and 12.55 (s, 2H), 7.80 (s, 4H), 7.25−7.65 (m, 18H). IR (KBr) ν_{max}: 3416, 3050, 1602, 1584, 1574, 1509, 1480, 1457, 1138, 1081, 970, 900, 850, 789, 768, 772, 713, 696, 681, 614 cm^{-1}. FAB MS (*m*/*z*): $[M + H]^+$ calcd for $C_{36}H_{24}Cl_2N_4$, 583.52; found, 583.

(ii) To a solution of Cl-BDPI-4Y-lophine (0.200 g, 0.34 mmol) in benzene (300 mL) containing aqueous potassium hydroxide (2 N, 200 mL) was added potassium ferricyanide

(10.0 g, 25.3 mmol) in a period of 0.5 h. After addition of potassium ferricyanide, the organic layer became a blue solution from a colorless solution. The reaction mixture was stirred for an additional 2 days at room temperature. The organic layer was separated, washed with water, dried over calcium chloride, and concentrated to give Cl-BDPI-4Y as a black-purple powder. Recrystallization from hot benzene gave Cl-BDPI-4Yin 56% yield (0.112 g) as deep greenish-blue microcrystals with metallic luster. IR (KBr) ν_{max}: 3061, 2925, 2854, 1724, 1587, 1564, 1522, 1483, 1442, 1344, 1277, 1236, 1181, 1132, 1069, 1028, 920, 850, 739, 698, 650 cm^{-1}. Anal. Calcd for $C_{36}H_{22}Cl_2N_4$: C, 74.36; H, 3.81; N, 9.64. Found: C, 74.06; H, 4.01; N, 9.35.

1,4-Bis[2-(2,6-dichlorophenyl)-5-phenylimidazol-4-ylidene]-cyclohexa-2,5-diene (dCl-BDPI-4Y). (i) Under nitrogen, to a stirred solution of 2,6-dichlorobenzalaldehyde (1.00 g, 5.71 mmol), 1,4-bisbenzil (1.00 g, 2.92 mmol) and ammonium acetate (5.00 g, 64.8 mmol) in acetic acid (100 mL) were heated to reflux, giving a light yellow and clear solution. After being refluxed for 2 days, the reaction mixture was cooled to room temperature and then added dropwise to an ice 10 % ammonia solution. It immediately formed a pale-yellow precipitate, which was collected by filtration and washed with water and then ethanol. Recrystallization of the pale-yellow product from pyridine gave 1,4-bis[2-(2,6-dichlorophenyl)-5-phenyl-imidazol-4-yl)benzene (dCl-BDPI-4Y-lophine) in 68% yield (1.29 g) as a white powder. ^{1}HNMR (DMSO-d_6, 500 MHz): δ 12.76, 12.78, 12.82 and 12.86 (s, 2H), 7.80 (s, 4H), 7.22−7.67 (m, 16H). IR (KBr) ν_{max}: 3381, 3070, 1602, 1559, 1510, 1477, 1435, 1387, 1193, 970, 843, 789, 778, 698 cm^{-1}. FAB MS (*m*/*z*): $[M + H]^+$ calcd for $C_{36}H_{22}Cl_4N_4$, 652.40; found, 653. Anal. Calcd for $C_{36}H_{22}Cl_4N_4$: C, 66.28; H, 3.40; N, 8.59. Found: C, 66.39; H, 3.28; N, 8.42.

(ii) To a solution of dCl-BDPI-4Y-lophine (1.00 g, 1.53 mmol) in benzene (250 mL) containing aqueous potassium hydroxide (2 N, 200 mL) was added potassium ferricyanide (18.0 g, 25.3 mmol) in a period of 0.5 h. After addition of potassium ferricyanide, the organic layer became a blue solution from a colorless solution. The reaction mixture was stirred for an additional 2 days at room temperature. The organic layer was separated, washed with water, dried over calcium chloride, and concentrated to give dCl-BDPI-4Y as black-purple powder. Recrystallization from hot benzene gave dCl-BDPI-4Y in 51% yield (0.505 g) as black microcrystals with metallic luster. IR (KBr) ν_{max}: 3064, 2925, 1599, 1560, 1472, 1431, 1344, 1321, 1268, 1194, 1161, 1124, 1024, 922, 854, 779, 698, 679, 551 cm^{-1}. Anal. Calcd for $C_{36}H_{20}Cl_4N_4(C_6H_6)_2$: C, 71.47; H, 4.00; N, 6.95. Found: C, 71.15; H, 4.04; N, 6.94.

Theoretical Methods. All calculations were carried out using the Gaussian 03 program.[7] The geometries of all molecules were fully optimized, and analytical second derivatives were computed using vibrational analysis to confirm each stationary point to be a minimum using the 6-31G(d) basis set and B3LYP hybrid density functional theory (DFT). Relative energies were corrected after zero-point energies (ZPE) were scaled by 0.9804. Spin-unrestricted B3LYP (UB3LYP) theory was used for triplet states, while both spin-restricted (RB3LYP) and UB3LYP methods were employed for singlet states. Especially, UB3LYP calculations (Guess=Mix) in broken symmetry (BS) were performed for the singlet biradical states of the compounds. The BS approach is a powerful tool for handling molecules with internal instabilities in their wave functions as the singlet biradical states of molecules.[8] The unrestricted Kohn−Sham wave functions obtained from SCF calculations are eigenfunctions of the S_z operator but are not eigenfunctions of the S^2 operator. Consequently, the shortcoming of this approach is that the BS wave functions of the singlet state are often spin-contaminated by higher multiplicity states. For the wave functions of singlet states, the spin contamination is exhibited by nonzero values of the spin-squared expectation value, $\langle S^2 \rangle = S(S + 1)$, where S is the molecular spin quantum number. However, the spin contaminations of our results are not so large. In the BS singlet states, the spin-squared expectation values $\langle S^2 \rangle$ have a narrower range of values ranging from 0.0192 to 0.1275. The spin contaminations of the triplet states are negligibly small. Therefore, we did not employ the spin-projected methods to eliminate the redundant spin contamination from the energies of the triplet and the BS singlet states.

3. Results and Discussion

BDPI-4Y derivatives are stable in benzene even at room temperature as well as lophyl radicals and BDPI-2Y. The solutions of BDPI-4Y derivatives show deep-blue color in most of the organic solvents, although the color of the solution gradually faded in all but the benzene solution. This fading may be attributable to hydrogen abstraction from solvent by radical species. Absorption spectra of BDPI-4Y derivatives in benzene are shown in Figure 1. The absorption spectrum of Cl-BDPI-4Y is slightly blue shifted as compared to that of BDPI-4Y, indicating the similarity in the electronic structures between these two compounds. On the other hand, the absorption maximum of dCl-BDPI-4Y is largely shifted to shorter wavelength more than 140 nm accompanying a large decrease in the molar extinction coefficient. The large blue shift in the absorption spectrum indicates the shortening of π-conjugation length. From the variation in the absorption spectra of BDPI-4Y derivatives, the changes in the energy gap between the diamagnetic ground state and the paramagnetic excited triplet state affecting a spin concentration were expected.

The toluene solution of BDPI-4Y derivatives shows an ESR signal consisting of a moderately broad unresolved line, ΔH_{pp} (peak-to-peak line width) $\approx$ 1 mT, at room temperature. Spin concentration was determined by carefully integrating the ESR signal in comparison with that of the DPPH solution as a standard. At room temperature, the spin concentration of BDPI-4Y, Cl-BDPI-4Y, and dCl-BDPI-4Y are 7.90×10^{21}, 1.17×10^{22}, 0.93×10^{21} spin/mol, respectively. The temperature dependence of ESR intensities in toluene solution is shown in Figure 2. The ΔH_{pp} values are almost constant at the measured temperature range. The ESR intensities decrease upon cooling

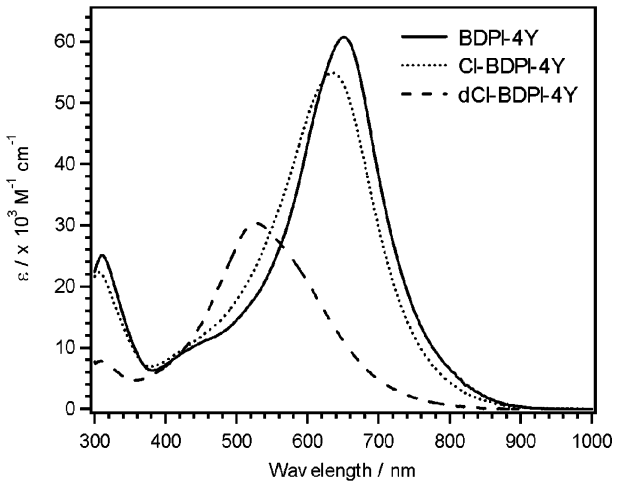

Figure 1. Absorption spectra of BDPI-4Y derivatives in benzene (2.5×10^{-5} M).

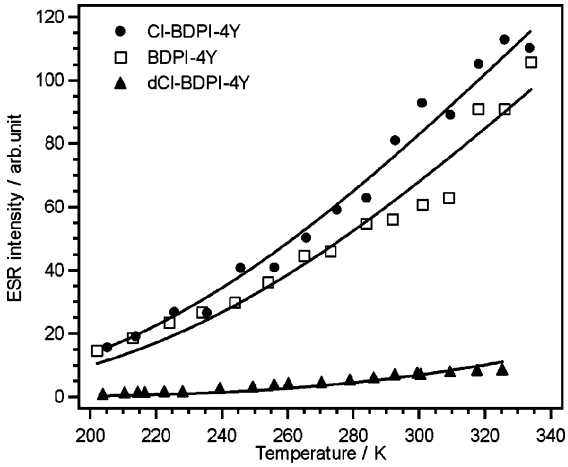

Figure 2. Temperature dependence of ESR signal intensities of BDPI-4Y derivatives in toluene solution (3.0×10^{-4} M). The solid lines represent the fit to the Bleaney−Bowers equation for the two-site Hisenberg Hamiltonian.

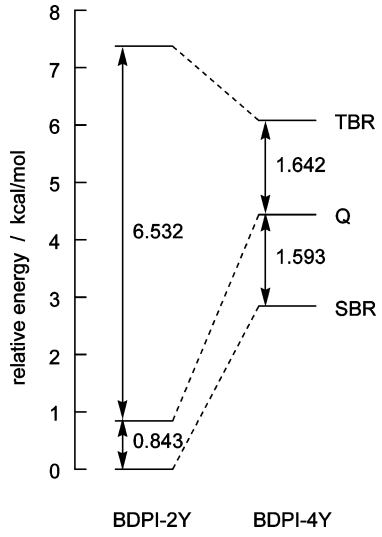

Figure 3. Energy level diagrams of BDPI-2Y and BDPI-4Y calculated by the DFT B3LYP/6-31G(d).

to low temperatures. The intensity behavior is reproducible as a function of cycling the temperature between 200 and 330 K and is attributable to the anti-Curie law behavior from equilibration of thermally populated triplet state species with slightly more stable ESR-silent singlet state species. Quantitative determination of the singlet−triplet energy gap is carried out by analyzing the ESR signal intensity based on the Bleaney−Bowers equation for the two-site Hisenberg Hamiltonian, $H = -2JS_1 \cdot S_2$.[9] The energy gaps between the singlet and the thermally excited triplet states for BDPI-4Y, Cl-BDPI-4Y, and dCl−BDPI-4Y are determined as 2.80, 2.68, and 4.17 kcal/mol, respectively.

Figure 3 shows the energy level diagrams of BDPI-2Y and BDPI-4Y obtained from the DFT calculations. The energy differences, ΔE(SBR−Q), between the open-shell broken-symmetry singlet and the closed-shell RB3LYP singlet were found. Pople and co-workers have suggested that the difference in energies between the closed-shell (RHF) and open-shell (UHF) singlet wave functions provides an indication of relative biradical character.[10] The more the UHF singlet energy falls below that of the corresponding RHF quantity, the greater is the biradical character of the singlet state. Recently, the presence of an open-shell singlet biradical ground state for larger

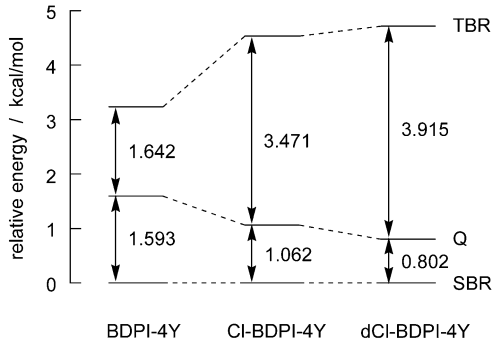

Figure 4. Energy level diagrams of BDPI-4Y derivatives calculated by the DFT B3LYP/6-31G(d). The energy levels of SBR state of all BDPI-4Y derivatives are set to zero for comparing the energy level differences for each molecule.

oligoacenes was predicted by the theoretical calculations.[11] The wave functions for polyacenes longer than hexacene were found to become unstable and develop into open-shell singlet biradicals as a result of their disjoint biradical character.[12] The energies of BDPI-2Y and BDPI-4Y can be compared using the same energy scale, because they are structural isomers. Accordingly, the energy level of the SBR state of BDPI-2Y was set to the origin of the energy axis in Figure 3. The closed-shell singlet quinoidal (Q) states are 0.843 and 1.593 kcal/mol above the SBR states for BDPI-2Y and BDPI-4Y, respectively. Therefore, it is suggested that the biradical character in the ground state of BDPI-4Y is greater than that of BDPI-2Y. The energy level of the SBR state of BDPI-4Y lies 2.845 kcal/mol above that of BDPI-2Y. For BDPI-4Y, both the deviation from planarity of two imidazolyl rings and the central phenylene ring, and the difficulty to take quinoidal structure, would cause the destabilization of the Q state. On the other hand, this structural change induces the stabilization of the energy level of the triplet biradical (TBR) state of BDPI-4Y. The detail of molecular structures for each state will be described later. The energy gap between the TBR state and the SBR state of BDPI-4Y is calculated to be 3.235 kcal/mol, which is much smaller than the corresponding value of 7.375 kcal/mol for BDPI-2Y. The decrease in the energy gap between the singlet state and the triplet state is consistent with the spin concentrations of the thermally populated triplet state determined by the ESR measurements. On the other hand, the energy level of Cl-BDPI-4Y and dCl-BDPI-4Y cannot be compared directly with those of BDPI-2Y and BDPI-4Y in the same energy scale. The energy levels of the SBR state of all BDPI-4Y derivatives were set to zero, and the relative energy levels were displayed in Figure 4. As was expected from the ESR measurements, the increase in the energy gap between the singlet state and the triplet state of dCl-BDPI-4Y was also confirmed by the calculations. The largest values of ΔE(SBR−Q) and $\langle S^2 \rangle$ for the SBR state of BDPI-4Y are suggestive of the increase in the biradical character of the singlet ground state among BDPI derivatives (Table 1).

To obtain more detailed insight into the nature of the electronic structures for the molecules, frontier molecular orbitals (MOs) and spin-density distributions were investigated. Figure 5 shows the SOMO and the spin-density distribution of lophyl radical, which can be regarded as a half unit of BDPI derivatives. Spin delocalization over the whole region of the molecule was revealed from the SOMO and the spin-density distribution. By considering a pentagonal shape of the imidazolyl ring, it is quite natural that an alternating pattern of spin densities as the spin polarization effect is violated in the imidazolyl ring. Frontier MOs of BDPI-4Y are shown in Figure 6. At a glance, these

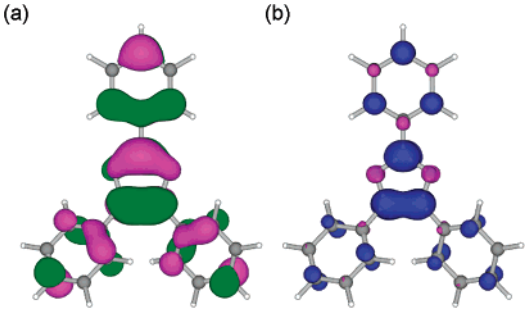

Figure 5. (a) SOMO and (b) spin-density distribution of triphenylimidazolyl radical.

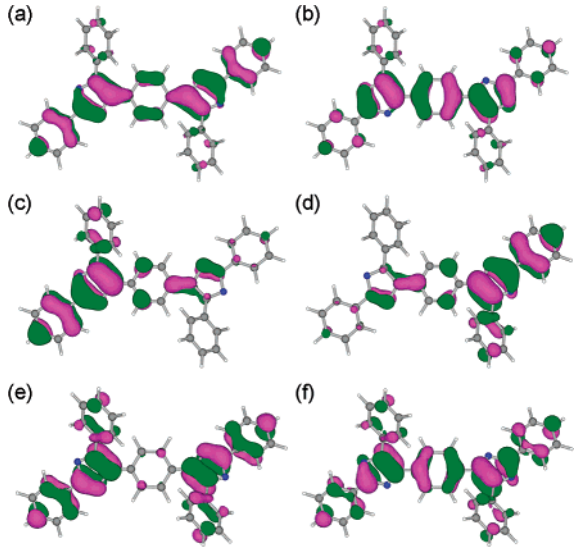

Figure 6. (a) HOMO (MO 134) and (b) LUMO (MO 135) of Q state, (c) SOMO (MO 134α) and (d) SOMO (MO 134β) of SBR state, and (e) SOMO (MO 134α) and (f) SOMO (MO 135α) of TBR state of BDPI-4Y.

frontier MOs are found to be constructed from the SOMOs of lophyl radicals. The HOMO and LUMO of the Q state are similar to the two SOMOs of the TBR state in the spatial distributions and the symmetrical features. On the other hand, the two SOMOs of the SBR state have asymmetrical distributions with a disjoint character. From the standpoint of the Hartree−Fock self-consistent field (SCF) theory based on the variation principle, the SCF MOs are determined to minimize the total electronic energy of molecules. Therefore, the SOMOs of the SBR state are found to show a disjoint character described above, because the two unpaired electrons would be distributed to different sets of atoms in molecule to minimize the Coulombic repulsion energy arising from electrons of opposite spin.[13]

The spin-density distributions for the SBR and TBR states for BDPI-2Y are shown in Figure 7, and those for BDPI-4Y and dCl-BDPI-4Y are shown in Figure 8. Despite that the unpaired electron spins in the TBR state of BDPI-2Y distribute

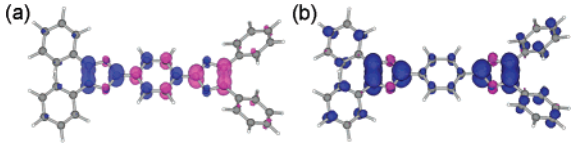

Figure 7. Spin-density distributions of (a) SBR state and (b) TBR state of BDPI-2Y.

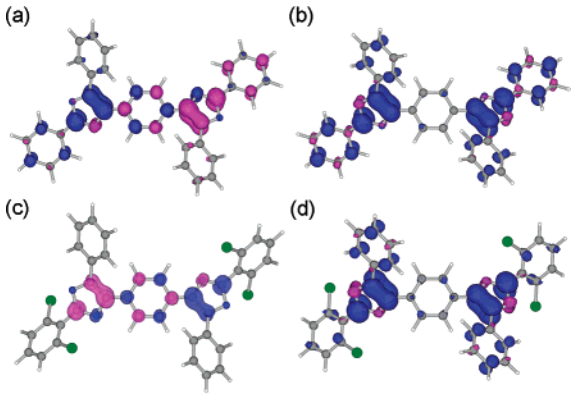

Figure 8. Spin-density distributions of (a) SBR and (b) TBR states of BDPI-4Y, and (c) SBR and (d) TBR states of dCl-BDPI-4Y.

in the central phenylene ring, very low spin-densities are found in those of BDPI-4Y and dCl-BDPI-4Y. This spin-density distribution manner is anticipated to be important in stabilizing the energy level of the TBR states for BDPI-4Y derivatives. Moreover, by comparing the spin-density distribution of BDPI-4Y (Figure 9) with that of dCl-BDPI-4Y, a significant decrease in the degree of penetration over the terminal phenylene rings is confirmed. These diversities in the spin-density distributions can be easily understood by referencing molecular structures. The two chlorine atoms introduced in the terminal phenylene rings of dCl-BDPI-4Y would increase the dihedral angle between the imidazolyl ring and the terminal phenylene ring. This shortening of the π-conjugation length is also consistent with the large blue shift in the absorption maximum accompanied by the large decrease in the molar extinction coefficient as shown in Figure 1. Therefore, the penetration of electron spins into the terminal phenylene ring is considered to be prevented by this structural change. The confinement of electron spins in the imidazolyl ring increases the Coulomb repulsion in the triplet biradical state of dCl-BDPI-4Y. Therefore, the energy gap between the singlet state and the triplet state of dCl-BDPI-4Y would be enlarged as compared to that of BDPI-4Y as suggested from the temperature dependence of ESR intensities.

The molecular geometries of the Q, SBR, and TBR states of BDPI-4Y are listed in Table 2. An important feature of molecular structure is represented by the bond lengths of C2−C3, C4−C5, and N1−C7. These bond lengths gradually lengthen from the Q state to the TBR state, indicating the structural change of the central phenylene ring from quinoidal

TABLE 1: Hartree−Fock Energies (hartrees) of Q State, SBR State, and TBR State, Unscaled Zero-Point Energy (ZPE) Corrections, and Spin-Squared Expectation Values $\langle S^2 \rangle$ Calculated by the DFT UB3LYP/6-31G(d) Method

		BDPI-2Y	BDPI-4Y	Cl-BDPI-4Y	dCl-BDPI-4Y
Q	E_{HF}^{Q}	−1605.29032905	−1605.28458178	−2524.45704934	−3443.62490193
	ZPE^{Q}	0.503869	0.503851	0.484026	0.463850
SBR	E_{HF}^{SBR}	−1605.29078245	−1605.28595547	−2524.45760957	−3443.62506354
	ZPE^{SBR}	0.502962	0.502663	0.482871	0.462711
	$\langle S^2 \rangle$	0.0295	0.1275	0.0570	0.0192
TBR	E_{HF}^{TBR}	−1605.27831390	−1605.28065477	−2524.45013791	−3443.61702483
	ZPE^{TBR}	0.502232	0.502515	0.482619	0.462179
	$\langle S^2 \rangle$	2.0006	2.0009	2.0007	2.0008

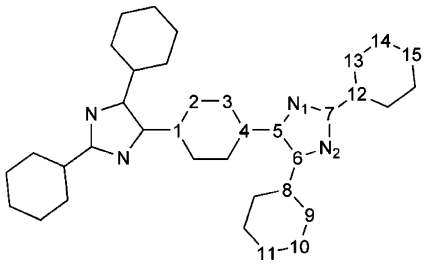

Figure 9. The atom labeling of BDPI-4Y.

TABLE 2: Selected Bond Lengths (Å) and Dihedral Angles (deg) for Q State, SBR State, and TBR State of BDPI-4Y Calculated by the DFT UB3LYP/6-31G(d) Method

	Q state	SBR state	TBR state
C1−C2	1.436	1.423	1.410
C2−C3	1.365	1.376	1.388
C3−C4	1.438	1.424	1.409
C4−C5	1.409	1.434	1.465
C5−C6	1.487	1.488	1.486
C5−N1	1.370	1.352	1.329
N1−C7	1.327	1.344	1.373
N2−C7	1.399	1.387	1.365
C6−N2	1.315	1.321	1.333
C6−C8	1.471	1.469	1.462
C8−C9	1.407	1.408	1.411
C9−C10	1.392	1.391	1.390
C10−C11	1.398	1.398	1.399
C7−C12	1.455	1.451	1.446
C12−C13	1.409	1.410	1.411
C13−C14	1.390	1.390	1.390
C14−C15	1.400	1.400	1.400
C3−C4−C5−N1	11.5	16.0	29.0
N2−C6−C8−C9	39.6	35.8	27.7
N1−C7−C12−C13	0.8	0.3	0.0

structure to biradical structure as illustrated in Scheme 1c. Another important feature of molecular structure is found in the changes in the dihedral angle defined by C3−C4−C5−N1. The angle in the TBR state (29.0°) is about 3 times that in the Q state (11.5°). The corresponding dihedral angles of BDPI-2Y in the Q state and the TBR state are 0° and 2.0°, respectively. Thus, it could be concluded that the deviation from the planarity in BDPI-4Y as compared to BDPI-2Y may stabilize the energy level of the TBR state and destabilize that of the Q state.

4. Conclusion

We have developed a new family of π-conjugated delocalized biradical compound, BDPI-4Y, which is a structural isomer of BDPI-2Y. The presence of the thermal equilibrium between a triplet biradical state and a singlet state was confirmed by the ESR measurements. The significant increase in the spin concentration was achieved by the geometrical recombination inducing the destabilization of the quinoidal state. The DFT calculations predicted the presence of the open-shell disjoint biradical ground state for BDPI-4Y and their halogenated derivatives Cl-BDPI-4Y and dCl-BDPI-4Y. We believe the materials with the biradical character in a ground state will lead to a novel development of molecule-based organic magnets.

Acknowledgment. This work was partially supported by a Grant-in-Aid for the 21st Century COE Program from MEXT, Japan. A.K. is grateful for financial support via a Grant-in-Aid for JSPS Fellows from MEXT, Japan.

References and Notes

(1) (a) Hayashi, T.; Maeda, K. *Bull. Chem. Soc. Jpn.* **1960**, *33*, 565−566. (b) Hayashi, T.; Maeda, K. *Bull. Chem. Soc. Jpn.* **1962**, *35*, 2057−2058. (c) Hayashi, T.; Maeda, K.; Morinaga, M. *Bull. Chem. Soc. Jpn.* **1964**, *37*, 1563−1564. (d) Hayashi, T.; Maeda, K.; Takeuchi, M. *Bull. Chem. Soc. Jpn.* **1964**, *37*, 1717−1718. (e) Hayashi, T.; Maeda, K.; Kanaji, T. *Bull. Chem. Soc. Jpn.* **1965**, *38*, 857−858. (f) Hayashi, T.; Maeda, K. *Bull. Chem. Soc. Jpn.* **1965**, *38*, 685−686. (g) Hayashi, T.; Maeda, K. *Bull. Chem. Soc. Jpn.* **1967**, *40*, 2990. (h) Maeda, K.; Hayashi, T. *Bull. Chem. Soc. Jpn.* **1970**, *43*, 429−438. (i) Maeda, K.; Hayashi, T. *Bull. Chem. Soc. Jpn.* **1969**, *42*, 3509−3514. (j) Shida, T.; Maeda, K.; Hayashi, T. *Bull. Chem. Soc. Jpn*. **1970**, *43*, 652−657.

(2) (a) White, D. M.; Sonnenberg, J. *J. Am. Chem. Soc.* **1966**, *88*, 3825−3829. (b) Cohen, R. *J. Org. Chem.* **1971**, *36*, 2280−2284. (c) Riem, R. H.; MacLachlan, A.; Coraor, G. R.; Urban, E. J. *J. Org. Chem.* **1971**, *36*, 2272−2275. (d) Cescon, L. A.; Coraor, G. R.; Dessauer, R.; Silversmith, E. F.; Urban, E. J. *J. Org. Chem.* **1971**, *36*, 2262−2267. (e) Tanino, H.; Kondo, T.; Okada, K.; Goto, T. *Bull. Chem. Soc. Jpn.* **1972**, *45*, 1474−1480. (f) Goto, T.; Tanino, H.; Kondo, T. *Chem. Lett.* **1980**, 431−434. (g) Lavabre, D.; Levy, G.; Laplante, J. P.; Micheau, J. C. *J. Phys. Chem.* **1988**, *92*, 16−18. (h) Qin, X.-Z.; Liu, A.; Trifunac, A. D.; Krongauz, V. V. *J. Phys. Chem.* **1991**, *95*, 5822−5826. (i) Liu, A.; Trifunac, A. D.; Krongauz, V. V. *J. Phys. Chem.* **1992**, *96*, 207−211. (j) Lin, Y.; Liu, A.; Trifunac, A. D.; Krongauz, V. V. *Chem. Phys. Lett.* **1992**, *198*, 200−206. (k) Morita, H.; Minagawa, S. *J. Photopolym. Sci. Technol.* **1992**, *5*, 551−556. (l) Monroe, B. M.; Weed, G. C. *Chem. Rev.* **1993**, *93*, 435−448. (m) Weidong, Y.; Yongyuan, Y.; Junshen, W.; Cunlin, Z.; Meiwen, Y. *J. Photopolym. Sci. Technol.* **1994**, *7*, 1870−192. (n) Ma, S.; Nebe, W. J. *J. Imaging Sci. Technol.* **1993**, *37*, 498−504. (o) Caspar, J. V.; Khudyakov, I. V.; Turro, N. J.; Weed, G. C. *Macromolecules* **1995**, *28*, 636−641. (p) Oliver, E. W.; Evans, D. H.; Caspar, J. V. *J. Electroanal. Chem.* **1996**, *403*, 153−158. (q) Okada, K.; Imamura, K.; Oda, M.; Kozaki, M.; Morimoto, Y.; Ishino, K.; Tashiro, K. *Chem. Lett.* **1998**, 891−892. (r) Kikuchi, A.; Iyoda, T.; Abe, J. *Chem. Commun.* **2002**, 1484−1485. (s) Nakahara, I.; Kikuchi, A.; Iwahori, F.; Abe, J. *Chem. Phys. Lett.* **2005**, *402*, 107−110.

(3) (a) Kawano, M.; Sano, T.; Abe, J.; Ohashi, Y. *J. Am. Chem. Soc.* **1999**, *121*, 8106−8107. (b) Abe, J.; Sano, T.; Kawano, M.; Ohashi, Y.; Matsushita, M. M.; Iyoda, T. *Angew. Chem., Int. Ed.* **2001**, *40*, 580−582. (c) Kawano, M.; Sano, T.; Abe, J.; Ohashi, Y. *Chem. Lett.* **2000**, 1372−1373.

(4) Mayer, U.; Baumgärtel, H.; Zimmermann, H. *Angew. Chem.* **1966**, *78*, 303.

(5) (a) Sakaino, Y.; Hayashi, T.; Maeda, K. *Nippon Kagaku Kaishi* **1972**, 100−103. (b) Sakaino, Y.; Kakisawa, H.; Kusumi, T.; Maeda, K. *J. Org. Chem.* **1979**, *44*, 1241−1244. (c) Sakaino, Y. *J. Chem. Soc., Perkin Trans. 1* **1983**, 1063−1066.

(6) Kikuchi, A.; Iwahori, F.; Abe, J. *J. Am. Chem. Soc.* **2004**, *126*, 6526−6527.

(7) Frisch, M. J.; Trucks, G. W.; Schlegel, H. B.; Scuseria, G. E.; Robb, M. A.; Cheeseman, J. R.; Montgomery, J. A., Jr.; Vreven, T.; Kudin, K. N.; Burant, J. C.; Millam, J. M.; Iyengar, S. S.; Tomasi, J.; Barone, V.; Mennucci, B.; Cossi, M.; Scalmani, G.; Rega, N.; Petersson, G. A.; Nakatsuji, H.; Hada, M.; Ehara, M.; Toyota, K.; Fukuda, R.; Hasegawa, J.; Ishida, M.; Nakajima, T.; Honda, Y.; Kitao, O.; Nakai, H.; Klene, M.; Li, X.; Knox, J. E.; Hratchian, H. P.; Cross, J. B.; Adamo, C.; Jaramillo, J.; Gomperts, R.; Stratmann, R. E.; Yazyev, O.; Austin, A. J.; Cammi, R.; Pomelli, C.; Ochterski, J. W.; Ayala, P. Y.; Morokuma, K.; Voth, G. A.; Salvador, P.; Dannenberg, J. J.; Zakrzewski, V. G.; Dapprich, S.; Daniels, A. D.; Strain, M. C.; Farkas, O.; Malick, D. K.; Rabuck, A. D.; Raghavachari, K.; Foresman, J. B.; Ortiz, J. V.; Cui, Q.; Baboul, A. G.; Clifford, S.; Cioslowski, J.; Stefanov, B. B.; Liu, G.; Liashenko, A.; Piskorz, P.; Komaromi, I.; Martin, R. L.; Fox, D. J.; Keith, T.; Al-Laham, M. A.; Peng, C. Y.; Nanayakkara, A.; Challacombe, M.; Gill, P. M. W.; Johnson, B.; Chen, W.; Wong, M. W.; Gonzalez, C.; Pople, J. A. *Gaussian 03*, revision C.01; Gaussian, Inc.: Wallingford, CT, 2004.

(8) (a) Noodleman, L. *J. Chem. Phys.* **1981**, *74*, 5737−5743. (b) Norman, J. G.; Ryan, P. B.; Noodleman, L. *J. Am. Chem. Soc.* **1980**, *102*, 4279−4282. (c) Noodleman, L.; Norman, J. G. *J. Chem. Phys.* **1979**, *70*, 4903−4906.

(9) Bleaney, B.; Bowers, K. D. *Proc. R. Soc. London, Ser. A* **1952**, *214*, 451−465.

(10) Kahn, S. D.; Hehre, W. J.; Pople, J. A. *J. Am. Chem. Soc.* **1987**, *109*, 1871−1873.

(11) Bendikov, M.; Duong, H. M.; Starkey, K.; Houk, K. N.; Carter, E. A.; Wudl, F. *J. Am. Chem. Soc.* **2004**, *126*, 7416−7417.

(12) Norton, J. E.; Houk, K. N. *J. Am. Chem. Soc.* **2005**, *127*, 4162−4163.

(13) (a) Borden, W. T.; Davidson, E. R. *J. Am. Chem. Soc.* **1977**, *99*, 4587−4594. (b) Borden, W. T.; Iwamura, H.; Berson, J. A. *Acc. Chem. Res.* **1994**, *27*, 109−116. (c) McMasters, D. R.; Wirz, J. *J. Am. Chem.* Soc. **2001**, *123*, 238−246. (d) Houk, K. N.; Lee, P. S.; Nendel, M. *J. Org. Chem.* **2001**, *66*, 5517−5521.